

AD-A099 272 SPECTROLAB INC SYLMAR CALIF  
LOW RESISTIVITY - HIGH LIFETIME SINGLE CRYSTAL SILICON INVESTIGATE ETC(U)  
MAR 81 J FODOR, R W OPJORDEN F33615-77-C-2045

UNCLASSIFIED

AFWAL-TR-81-2013

F A 2045

NL

| OF |  
AD  
90 99272

END  
DATE  
10-81  
DTIC

~~LEVEL II~~

(2)

AFWAL-TR-81-2013

ADA099272



## LOW RESISTIVITY — HIGH LIFETIME SINGLE CRYSTAL SILICON INVESTIGATION

SPECTROLAB, INC.  
12500 GLADSTONE AVENUE  
SYLMAR, CALIFORNIA 91342

MARCH 1981

TECHNICAL REPORT AFWAL-TR-81-2013  
Final Report for period August 1977 – December 1980

Approved for public release; distribution unlimited.

DMC FILE COPY

AERO PROPULSION LABORATORY  
AIR FORCE WRIGHT AERONAUTICAL LABORATORIES  
AIR FORCE SYSTEMS COMMAND  
WRIGHT-PATTERSON AIR FORCE BASE, OHIO 45433

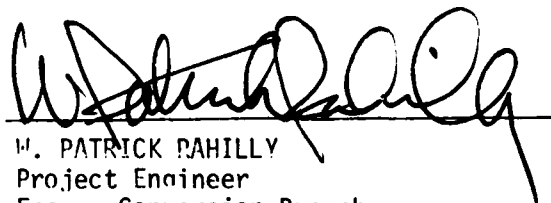
816 03051

NOTICE

When Government drawings, specifications, or other data are used for any purpose other than in connection with a definitely related Government procurement operation, the United States Government thereby incurs no responsibility nor any obligation whatsoever; and the fact that the government may have formulated, furnished, or in any way supplied the said drawings, specifications, or other data, is not to be regarded by implication or otherwise as in any manner licensing the holder or any other person or corporation, or conveying any rights or permission to manufacture use, or sell any patented invention that may in any way be related thereto.

This report has been reviewed by the Office of Public Affairs (ASD/PA) and is releasable to the National Technical Information Service (NTIS). At NTIS, it will be available to the general public, including foreign nations.

This technical report has been reviewed and is approved for publication.



W. PATRICK RAHILLY  
Project Engineer  
Energy Conversion Branch  
Aerospace Power Division



JOSEPH W. WISE  
TAM, Solar/Thermal Power  
Energy Conversion Branch  
Aerospace Power Division

FOR THE COMMANDER



JAMES D. REAMS  
Chief, Aerospace Power Division  
Aero Propulsion Laboratory

"If your address has changed, if you wish to be removed from our mailing list, or if the addressee is no longer employed by your organization please notify AFWAL/P00C, W-PAFB, OH 45433 to help us maintain a current mailing list".

Copies of this report should not be returned unless return is required by security considerations, contractual obligations, or notice on a specific document.  
AIR FORCE/56780/22 May 1981 - 150

SECURITY CLASSIFICATION OF THIS PAGE (When Data Entered)

REPORT DOCUMENTATION PAGE		READ INSTRUCTIONS BEFORE COMPLETING FORM
1. REPORT NUMBER <b>AFWAL-TR-81-2013</b>	2. GOVT ACCESSION NO. <b>110-AC22272</b>	3. PECI-ET'S CATALOG NUMBER
4. TITLE (and Subtitle) <b>LOW RESISTIVITY - HIGH LIFETIME SINGLE CRYSTAL SILICON INVESTIGATION</b>	5. TYPE OF REPORT & PERIOD COVERED Final August 1977—December 1980	
7. AUTHOR(s) <b>J. Fodor R. W. Opjorden</b>	8. PERFORMING ORG. REPORT NUMBER <b>F33615-77-C-2045</b>	
9. PERFORMING ORGANIZATION NAME AND ADDRESS <b>Spectrolab, Inc. 12500 Gladstone Avenue Sylmar CA 91342</b>	10. PROGRAM ELEMENT, PROJECT, TASK AREA & WORK UNIT NUMBERS <b>2308-53-01 61102F</b>	
11. CONTROLLING OFFICE NAME AND ADDRESS <b>Aero Propulsion Laboratory (AFWAL/POOC) Air Force Wright Aeronautical Laboratories Wright-Patterson AFB OH 45433</b>	12. REPORT DATE <b>March 1981</b>	
14. MONITORING AGENCY NAME & ADDRESS (if different from Controlling Office)	13. NUMBER OF PAGES <b>42</b>	
16. DISTRIBUTION STATEMENT (of this Report)  <b>Approved for public release; distribution unlimited.</b>	15. SECURITY CLASS. (of this report) <b>UNCLASSIFIED</b>	
17. DISTRIBUTION STATEMENT (of the abstract entered in Block 20, if different from Report)		
18. SUPPLEMENTARY NOTES		
19. KEY WORDS (Continue on reverse side if necessary and identify by block number) <b>Silicon Solar Cells High Purity Silicon Solar Cells Space Photovoltaic Power</b>		
20. ABSTRACT (Continue on reverse side if necessary and identify by block number)  <b>Results of recent studies at Spectrolab utilizing improved quality, low resistivity silicon material are presented. Crystal doping methods used include boron ion implantation, diborane gas, and elemental gallium doping. Nt/P solar cells were fabricated from these materials and then evaluated electrically, both beginning of life and after electron irradiation. Cells made from 0.17 ohm-cm Si:Ga material yielded the most impressive results, with open circuit voltages of 633 mV at 25°C, AMO. This float zone grown material also proved stable under photon irradiation post electron irradiation.</b>		

## FOREWARD

The authors would like to thank Peter Randtke of the Industrial Products Division of Hughes Aircraft Company for his efforts in the crystal growth phase of this program. We would also like to thank Bruce Anspaugh and Tetsuo Miyahara for the electron irradiations, Mark Gillanders for his technical assistance, and Nancy Neal for her help in the cell fabrication phase of this work.

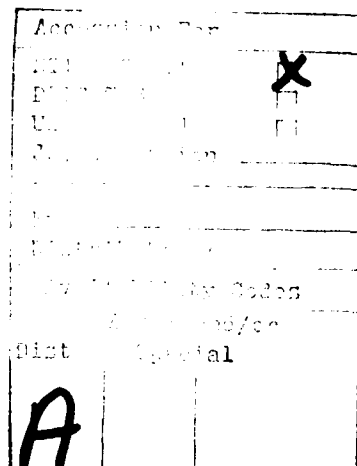


## TABLE OF CONTENTS

<u>Section</u>	<u>Title</u>	<u>Page</u>
1.0	Introduction	1
2.0	Technical Discussion	3
2.1	Introduction	3
2.2	Impurity Gettering	3
2.2.1	Phosphorous Diffusion Gettering	4
2.2.2	Aluminum Gettering	8
2.2.3	Gettering Summary	16
2.3	Crystal Growth	16
2.3.1	Starting Material	17
2.3.2	Doping and Crystal Growth	17
2.3.2.1	Ion Implantation	18
2.3.2.2	Diborane Doping	22
2.3.2.3	Gallium Doping	23
2.3.3	Crystal Growth Summary	25
2.4	Material Evaluations	27
2.4.1	Cell Processing	27
2.4.2	Electrical Evaluation	28
2.4.3	Electron Irradiation Tests	30
2.4.4	Photon Degradation Experiments	33
2.4.5	Material Evaluation Summary	33
2.5	Process Optimization - Gallium Doped Material	36
2.5.1	(100) Oriented Si:Ga Ingot	36
2.5.2	Electron Irradiation Test	37
3.0	Conclusion	40
	References	42

## LIST OF FIGURES

<u>Number</u>		<u>Page</u>
1	Spectral Response - Phosphorous Getter (900°C)	7
2	Spectral Response - Al (Evap.) Getter	10
3	Spectral Response - Al Getter (.05 ohm-cm silicon)	14
4	Normalized $I_{sc}$ vs Electron Fluence	34

## LIST OF TABLES

<u>Number</u>		<u>Page</u>
1	Ion Implant Ingot Characteristics	20
2	Doping Concentration	21
3	Lifetimes and Impurity Concentrations of Gallium Doped Ingots	24
4	List of Crystals	26
5	Average 25°C AMO Electrical Data Boron Doped Cells, 300 Microns Thick	29
6	Average AMO Electrical Data Gallium Doped Material, 300 Microns Thick	29
7	Electron Irradiation Data $3 \times 10^{14} \text{ e/cm}^2$ 1 MeV Electrons	31
8	Electron Irradiation Data $1 \times 10^{15} \text{ e/cm}^2$ 1 MeV Electrons	32
9	Photon Degradation Experiment Post $3 \times 10^{14}$ $\text{e/cm}^2$	35
10	25°C, AMO Test Data - (100), 2 ohm-cm Gallium Doped Material	38
11	25°C, AMO Electron Irradiation Data High Efficiency Cells	39

## 1.0 INTRODUCTION

In recent years silicon solar cell development programs have led to laboratory cells with AM0 conversion efficiencies of 16%.<sup>(1)</sup> Advances in photovoltaic technology have produced significant improvements in both short circuit current and curve fill factor, as well as improved voltage characteristics through refinements in back surface field technology. However, mathematical modeling has suggested that conversion efficiencies of 18% or better are possible using low resistivity (approximately 0.1 ohm-cm), single crystal silicon.<sup>(2)</sup> The major obstacle to the achievement of such high efficiencies has been the failure of cells produced from low resistivity silicon to achieve the theoretically predicted values of open circuit voltage. This has led to examinations of those variables which control  $V_{oc}$ .

The lower than predicted open circuit voltages for cells made from low resistivity material can be attributed to higher than normal values of the reverse saturation current.<sup>(3)</sup> This could be a result of high recombination currents caused by the inclusion of unwanted contaminants into the bulk silicon during crystal growth. These contaminants may then be gettered into the junction region during its formation. Since the higher doping levels of low resistivity material usually results in a higher contamination level as well, it is believed that the observed open circuit voltage deficiency could be attributed to these impurity induced recombination centers. Reducing the recombination current through improved purity material may be one method of improving cell open circuit voltage behavior.

It has also been theorized that the basic mechanism for radiation damage in silicon solar cells is the formation of recombination centers which result from interactions between radiation induced defects and the various impurities that are present in the silicon. Reduction of impurities in the bulk silicon may therefore not only yield improved cell efficiencies through open circuit voltage enhancement, but may also yield more radiation tolerant devices as well.

In this study several new methods of producing high purity, low resistivity single crystal silicon for solar cell use were investigated. These included:

- 1) Gettering of impurities from conventional, Czochralski grown silicon wafers.
- 2) Boron doping of high purity starting material using both boron ion implantation and gaseous diborane doping.
- 3) Float zoning silicon ingots under extremely clean conditions.
- 4) The use of gallium as the primary 'P' type dopant.

The resulting materials were then evaluated by measuring the electrical performance, both beginning of life and after electron irradiation, of solar cells produced from the new materials.

## 2.0 TECHNICAL DISCUSSION

### 2.1 INTRODUCTION

The objective of this program was to improve the performance of N<sup>+</sup>/P silicon solar cells by improving the minority carrier lifetime of moderate to low resistivity single crystal silicon material. In order to accomplish this goal various methods were developed to obtain single crystal silicon with very low levels of background impurities. Every effort was made to keep the concentration of all impurities other than the primary dopants at levels less than  $1 \times 10^{12}$  atoms/cm<sup>3</sup>. In order to evaluate these materials, solar cells were fabricated and then measured electrically under simulated air mass zero illumination. In addition, many of the materials were evaluated in terms of resistance to the effects of particle irradiations.

The technical effort was divided into the following four areas:

- 1) Impurity gettering
- 2) Crystal growth
- 3) Material evaluations
- 4) Process optimization

The results of these efforts are discussed in the following sections.

### 2.2 IMPURITY GETTERING

Gettering of impurities from silicon was considered as a possible alternative to growing ultra high purity doped silicon. The use of phosphorous and aluminum gettering sources was examined.

### 2.2.1 Phosphorous Diffusion Gettering

The phosphorous diffusion gettering was conducted with PH<sub>3</sub> gas. Twenty-four two ohm-cm boron doped, Czochralski grown wafers were used in the initial experiment. Sixteen of these wafers were subjected to an initial PH<sub>3</sub> diffusion of 30 minutes duration at 900°C. Based on the diffusion rates of the major lifetime damaging impurities such as gold and iron, this schedule was felt to offer sufficient time for gettering of contaminants.

The wafers at this point were in an as-sawn and cleaned (degreased) condition. It was not felt that a polished surface would enhance gettering and it was desirable to avoid potential staining that sometimes occurs when repeated etchings are done.

Following the PH<sub>3</sub> getter eight wafers had between 12 and 25 microns removed on each side with abrasive lapping. These wafers, the remaining eight gettered wafers, and an additional eight non-gettered wafers were then etched in a 30% NaOH solution to bring the final thicknesses to approximately 250 microns, corresponding to a loss of 150-200 microns of silicon. Since there was some concern regarding the redeposition of impurities from the etched-off silicon and etching solution back onto the silicon surface, all samples were then given a PNH clean.

The PNH cleaning technique uses a sequence of ammonium hydroxide, hydrogen peroxide, hydrochloric acid, and hydrofluoric acid, to provide a silicon wafer with a highly cleaned surface. It is reported that contaminants such as S and Cl are reduced to levels  $\sim 10^{13} \text{ cm}^{-2}$  and that impurities heavier than Cl occur at levels well below  $10^{12} \text{ cm}^{-2}$ .<sup>(4)</sup> This cleaning method has been used by Spectrolab for a number of years and proved to be quite effective in minimizing lifetime degradation occurring during the fabrication of boron BSF cells.<sup>(5)</sup>

Following the cleaning, all wafers were diffused at 825°C and then subjected to standard cell processing. The processing was stopped just before the AR coating step, since an AR coating might affect the results of subsequent spectral response measurements and complicate the determination of any bulk lifetime effects.

Although all groups of wafers started with the same initial thickness, the diffused surface was found to etch faster than non-diffused surfaces so that the gettered-and-not-lapped cells were thinnest at 9 mils, the controls were thickest at 11.9 mils, and the gettered and lapped wafers were 10.5 mils, the 1.4 mil reduction from the control case being the amount removed in lapping. As a result of the differences, corrections were made for thickness based on in-house work partially published in the Twelfth Photovoltaic Specialists Conference Record.<sup>(6)</sup> Corrected values of  $I_{sc}$  and  $V_{oc}$  at 25°C are shown below:

Cell Type	$I_{sc}$ (mA)	$V_{oc}$ (mV)
Control	104.2 ± 1.9	584 ± 3
PH <sub>3</sub> Gettered and* Etched	101.1 ± 1.6	588 ± 5
PH <sub>3</sub> Gettered, Lapped* and Etched	102.5 ± 1.3	585 ± 4

\*Data corrected for thickness effects

No gettering benefits were observed with all cell groups comparable in voltage and the control cells approximately 2% higher in  $I_{sc}$ , although all measurements are essentially equivalent within the degree of accuracy.

Spectral response measurements were then taken on the samples. A noticeable loss in long wavelength response was found for the PH<sub>3</sub> gettered cells (see Figure 1). Although some of this might be due to lifetime impairment in the gettered samples, it was felt that at least half of the difference in samples was due to the variation in sample thickness. As stated earlier the control samples were thickest at 300 microns, and the gettered and not-lapped wafers thinnest at 225 microns, and the gettered and lapped samples midway at 260 microns. These relative differences were reflected in the long wavelength spectral responses.

In order to minimize the impact of any degradation due to temperature, the PH<sub>3</sub> gettering was re-examined using a one half hour 850°C getter sequence. The 2 ohm-cm samples were prepared in a manner similar to the 900°C gettered samples, although the post getter silicon removal used NaOH etching without any lapping. In addition samples were etched so that test and control cells were of equal thicknesses (300 microns).

AMR measurements showed no significant differences between test and control samples. However, this time a slight advantage was observed for the gettered cells, although the difference was within the sample error limit. The I<sub>SC</sub> of the gettered cells was 104.3 mA compared to the I<sub>SC</sub> of the control samples which was 103.8 mA. The V<sub>OC</sub> was 585 ± 2 mV and 583 ± 3 mV for test and control cells respectively. The 850°C phosphorous gettered samples had higher currents than the 900°C phosphorous gettered samples, reflecting for the most part the thicker wafer size.

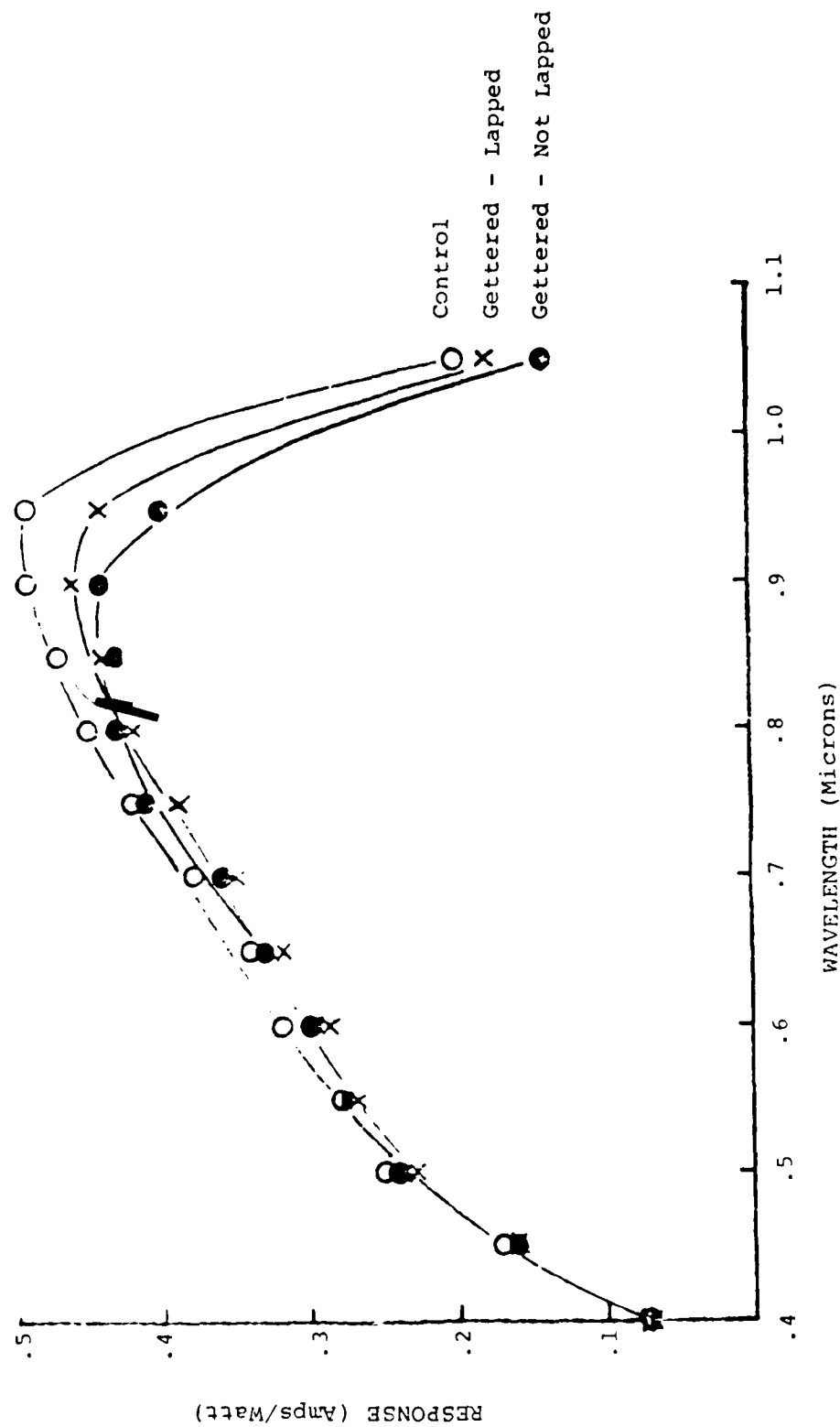


Figure 1 Spectral Response - Phosphorous Getter ( $900^{\circ}\text{C}$ )

Spectral response measurements also show the 850°C gettered and control cells to be essentially equivalent, with a slight (2%) advantage in response at 1.05 microns observed for the gettered samples. This is in contrast to the 900°C gettered cells where the samples had lower long wavelength responses than the control cells.

Spectral response curves for the 850°C gettered samples are not included since the data is essentially indistinguishable from the controls.

Analysis of the results of the phosphorous gettering work indicate that no advantage has been obtained. If anything, the importance of maintaining moderate processing temperatures is felt to have been demonstrated. Whereas a 900°C getter might be expected to remove more impurities than a 50°C lower getter, cell characteristics indicate a modest advantage in cell output is effected through the use of the lower processing temperature. The potential advantage of a phosphorous getter can be at best considered slight with gains falling within experimental accuracy limits.

#### 2.2.2 Aluminum Gettering

Following the phosphorous gettering work, a group of wafers was obtained for aluminum gettering studies; half were retained as controls and the remainder coated with approximately 6  $\mu\text{m}$  of evaporated aluminum. The aluminized wafers were alloyed at 850°C for 40 minutes, the excess aluminum residue was removed, and all wafers including controls were etched down 150-200 microns in 30% NaOH. Again, to prevent the redeposition of impurities all wafers were subjected to a PNH cleaning, followed by a PH<sub>3</sub> diffusion at 825°C, providing a sheet resistance of ~ 100 ohms per square.

Cells were fabricated in the normal manner, and measurements were obtained without AR coatings. Since the Al gettered wafers averaged 25 microns less in thickness, their values were corrected to compare with the 260 micron thick controls. AMO  $I_{sc}$  and  $V_{oc}$ , at 25°C were:

	$I_{sc}$	$V_{oc}$
Controls	103 ± 2 mA	584 ± 6 mV
Aluminum Gettered	100 ± 3 mA	577 ± 9 mV

These data indicate a slight loss for the gettered cells, similar to the work on PH<sub>3</sub> gettering, although all values are comparable within the experimental limits. A spectral response analysis indicated that the current difference resided in the medium and long wavelength regions. (Figure 2)

Following these initial results a second and similar evaporated Al getter was performed at 850°C, since spectral response measurements of the first evaporated Al getter samples had indicated a severe loss in mid and long wavelength spectral response, (see Figure 2) indicative of material lifetime degradation. The loss in response at 1.05 microns was approximately 35% with a nearly 20% loss evident at .9 microns. These values were quite in contrast to the smaller variations observed for PH<sub>3</sub> gettering. For this reason it was felt that it would be worthwhile repeating this experiment and an additional 8 controls and 8 samples were subjected to the same process. In this repeat test all cells were measured for electrical performance and spectral response, and no significant differences were observed between controls and gettered samples. At the same time it was not possible to identify any possible differences in the processing used for the first group of cells tested previously. It was noted that even after 30-70 microns have

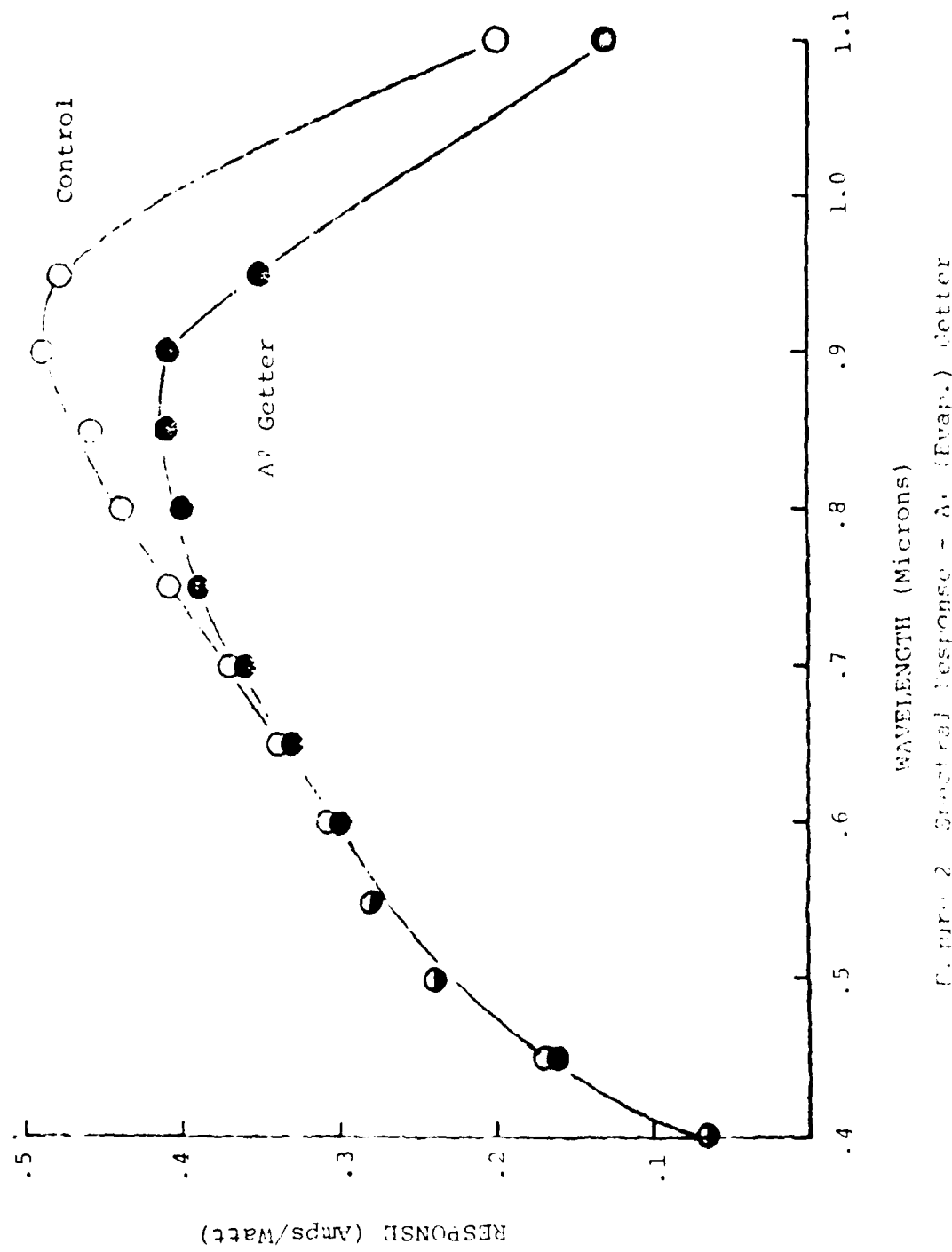


Fig. 2. Grayscale Response -  $\Delta$  (Evap.) Getter

been removed from each side of the Al gettered wafers, the gettered wafers can be identified from the controls by the appearance of bumps and pockets due to etching the uneven surface produced by the aluminum alloying. This might indicate the possibility of residual stresses in the silicon surfaces which might account for lifetime losses. However, the validity of this was greatly compromised by the fact that the second group of Al cells, which did not show any loss in lifetime, exhibited a significantly more eroded surface than the first group, which had the larger degradation. Although a specific degradation mechanism (introduction of impurities or stresses) cannot be defined by the limited data, it is interesting to propose that the performance of evaporated aluminum BSF cells may be compromised due to the introduction of lifetime degradation by the BSF process.

A third experiment was then conducted using a paste Al BSF process which has been very successful in cell fabrication. This tended to further indicate that the evaporated Al process can cause lifetime degradation. In this experiment Al paste was applied to a surface of the sample wafers and after drying, heated to 900°C for 20 minutes. The wafers were then etched in 30% NaOH to remove approximately 70 microns of silicon from each surface, PNH cleaned and fabricated into solar cells as before. The material for these samples was of slightly lower resistivity (1½ vs. 2 ohm-cm) than used with the evaporated Al cells, but this was not felt to be significant.

AM0 measurements showed the following characteristics:

	$I_{SC}$ (mA)	$V_{OC}$ (mV)
Al Paste Getter	102.3 ± 0.8	590 ± 3
Controls	102.5 ± 1.3	587 ± 1

The equivalency of output was reflected in the spectral response where no significant difference could be noted in any wavelength band from .4-.1.05 microns. At this point the aluminum getter work indicated (1) that no significant gettering enhancement had occurred, (2) that the higher temperature Al paste getter did not reduce bulk lifetime, and (3) that lifetime degradation may occur in the evaporated aluminum getter process.

Of all the gettering approaches, the Al paste process appeared to hold the greatest promise.

Consequently, a limited amount of 0.5 ohm-cm silicon material was made available for additional analysis of gettering. It was felt that the lower resistivity might exaggerate any gettering impact compared to the lower doped 2 ohm-cm material. Following the application and drying of the paste, the wafers were heated at 400°C for twenty minutes. It was noted that a number of wafers had regions of spalling due to the thermal expansion coefficient mismatch of the aluminum paste and the silicon which is apparently aggravated by the long heating cycle. Since the aluminum residue had approximately three mils of silicon were to be removed from the wafer surface in a nitric acid etch, it was not known if the spalling would cause any reliability problem. Hence, four samples were prepared to diffuse, anneal and proceed into seal. It turned out no significant electrical differences were noted between the spalled

and the non-spalled gettered samples, although the silicon thickness through the spalled region was approximately 25 microns less. Comparison to non-gettered 0.5 ohm-cm controls is shown below.

	$I_{SC}$ (mA)	$V_{OC}$ (mV)
Gettered	$104.5 \pm 1.0$	$583 \pm 7$
Control	$103.1 \pm 0.3$	$592 \pm 3$

As in previous tests, cell characteristics are for non-AR coated cells. The gain in  $I_{SC}$  for the gettered cells is 1.2% and although slight does appear real. The current gain is offset by a 1.5% loss in  $V_{OC}$ , which may be due to processing problems, since there is a large variation in the data. Spectral response data were obtained in order to characterize the nature of the current increase in the gettered samples. Figure 3 shows average spectral response for the gettered and control cells. Consistent with a gettering benefit to lifetime is a higher long wavelength response in the aluminum gettered cells, with a 7.5% gain at 0.95 microns.

These results were felt to indicate that the gettering process might be of some benefit to the lower resistivity material, although at present gains are quite minimal. In order to explore the process potential further, alternate gettering temperatures were examined. It is desirable to minimize high temperature excursions in cell fabrication since this lessens the possibility for lifetime damage, however, the removal of impurities by gettering is contingent on the mobility of the impurities in silicon which usually suggests that higher temperatures may be more practical.

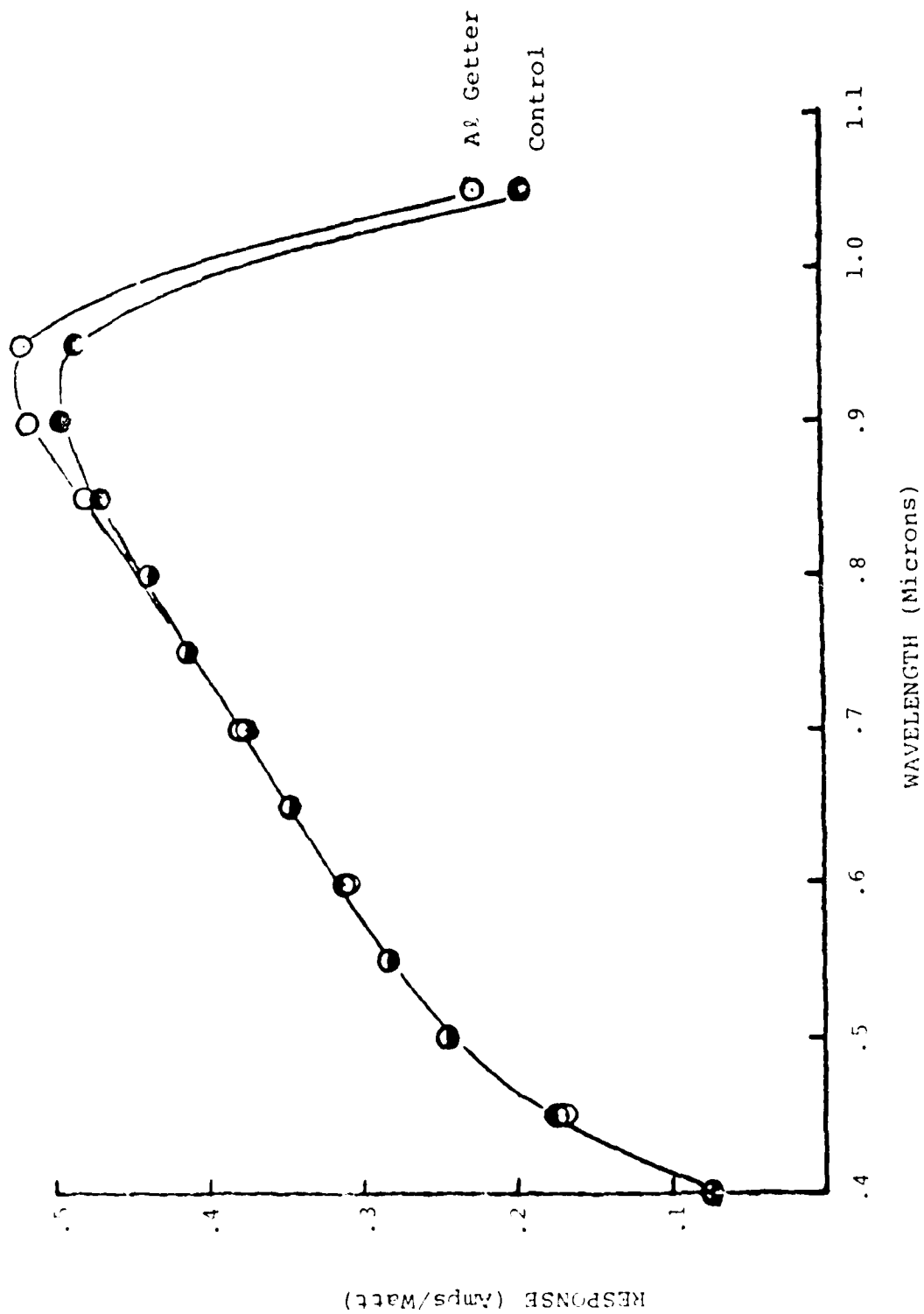


FIGURE 3 Spectral Response - Al Getter (.05 ohm-cm silicon)

For this reason three groups of wafers with aluminum paste were gettered at 800°C, 850°C, and 900°C for 20 minutes. This range was chosen to extend the range examined previously, and to comply with the reasonable temperature limits.

All wafers were nominal 1 ohm-cm silicon. Following the gettering the alloyed aluminum region was removed by hydroxide etching, along with approximately 70 microns of silicon from each side. Final wafer thickness was approximately 275 microns. A group of control wafers was etched down along with the gettered wafers, and all groups were fabricated together, in order to minimize fabrication variations.

Electrical results are shown below, this time for Ta<sub>2</sub>O<sub>5</sub> AR coated samples.

#### GETTERED CELL ELECTRICAL PERFORMANCE

Cell Type	I <sub>SC</sub> (mA)*	V <sub>OC</sub> (mV)	I@500 mV (mA)
800°C Getter	131.4 ± 2.4	600 ± 2	123.4 ± 2.9
850°C Getter	135.4 ± 1.2	602 ± 1	127.9 ± 2.2
900°C Getter	135 ± 1	602 ± 1	127.8 ± 1.5
Controls	134.7 ± 1.6	602 ± 1	127.7 ± 1.4

\*Approximately 8 wafers of each type

With the exception of the 800°C samples, all groups are equal. This is not too unexpected since it was proposed earlier that gettering would be more beneficial for lower resistivity material and since an approximate advantage of one percent had been noted for 0.5 ohm bulk silicon the lesser benefit on 1 ohm

is reasonable. The surprise is the performance of the 800°C getter samples which are appreciably lower than all other groups. Spectral response measurements show the loss to be in the mid and long wave regions. Since the aluminum paste used for gettering has been employed successfully for a BSF at the 800°C temperature, it is difficult to ascribe any specific mechanism to this anomaly. And since all wafers were processed together there is no reason to select any other step as the cause of the loss.

Possibly a significant quantity of impurities were collected toward the aluminum but were still 2-3 mils from it after the heating. They might then remain within the bulk near the back surface after silicon etching to degrade the cell output.

#### 2.2.3 Gettering Summary

Examination of gettering as a method of removing impurities from the silicon after ingot growth did not produce any significant improvement in cell performance. Of the three methods examined, only the aluminum paste technique produced cells which were consistently equal to or better than the control cells. It was not determined, however, whether this extra processing step had any beneficial effects on the bulk lifetime of the silicon wafers studied.

#### 2.3 CRYSTAL GROWTH

All single crystal, float zone grown "P" type material used in this work was supplied to Spectrolab by the Industrial Products Division of Hughes Aircraft Company (HAC-IPD). Hughes has developed the technology necessary for the growth of very high purity silicon for use as laser detectors, and it was felt that this expertise would benefit the present program as well.

### 2.3.1 Starting Material

The initial high purity polycrystalline silicon rod was prepared by Dow Corning. This rod was then vacuum float zoned under extremely clean conditions to form one inch diameter, pre-purified ingots. Boron levels for this material were typically kept below  $1 \times 10^{12}$  atoms/cm<sup>3</sup>, with all other impurities significantly below this as measured by the Hall effect as a function of temperature. Resistivity of the material was approximately 4000 ohm-cm, with lifetime ranging from 0.5 to 2 milliseconds.

### 2.3.2 Doping and Crystal Growth

Two "P" type dopants were selected for investigation, boron and gallium. Boron doping was performed by ion implantation of the pre-purified ingots or by the introduction of diborane ( $B_2H_6$ ) gas into the zoning chamber during crystal growth. Gallium doping was accomplished by the introduction of elemental gallium into the crystals during the zoning operation.

Early in the program a Siemen's model VZA-3 zoner was purchased by Hughes IPD from Westech, Inc. of Phoenix, Arizona. This unit, originally designated for float zone growth under vacuum, was modified with a new tank circuit and coil. In addition, the growth chamber was made suitable for positive pressure growth. An argon gas control and diborane doping system was likewise installed. Considerable care was given to providing cleanliness in the gas system by use of stainless steel fittings and spectroscopic purity gas. The plan was to use this furnace for final single crystal float-zone growth of the ion-implant, diborane doped and gallium doped ingots. However, difficulties

were encountered in using this furnace to grow zero defect crystals 1.25" in diameter, the size necessary for fabricating 2 cm x 2 cm solar cells. The major problem with the system was a poor match of the RF coil/tank circuit to the RF generator supplied with the system.

Several modifications were made on the system during the course of the program, including a new coil design and modifications in the tank circuit capacitor bank. Unfortunately these modifications were unsuccessful, and the furnace was not used in the final growth passes on any of the ingots. The VZA-3 zoner was only used for the diborane doping. Final growth passes on both the ion implanted and diborane doped ingots were performed by Hughes IPD personnel in a Westech system located at Great Western Silicon, Phoenix, Arizona. The gallium doped ingots were grown at Hughes Research Laboratories in Malibu, California.

#### 2.3.2.1 Ion Implantation

Boron implantation of the ingots was performed at Hughes Research Laboratories. Ion implantation is a method not commonly used in the doping of rods, but has proven to be a high purity method of forming junction layers in silicon slices. For the present study, a special jig was fabricated for holding the one inch diameter pre-purified ingots in the sample chamber of the implant apparatus. Boron implantation was performed using a boron trifluoride ( $BF_3$ ) source and an implantation energy of 100 KeV. Ingots were then regrown by vacuum float zoning to distribute the boron through the bulk of the crystal. Boron in silicon has a segregation coefficient near unity, hence the sweeping effect of the molten zone does not alter the boron distribution along the length of the ingot. Initially ingots of

0.2, 2, and 20 ohm-cm were attempted using  $B^+$  ions. In addition, one ingot was implanted using  $BF_2^+$  ions in order to investigate reported improvements using this species, both in the reduction of silicon damage during implantation, and in possible beneficial effects of the fluorine impurity on resultant cell characteristics.<sup>(7)</sup> All ingots were grown with (111) orientation.

Wafers were cut from the seed and tang ends of these initial implanted ingots for resistivity, Sirtl etch, lifetime and Hall measurements. A summary of the ingots' usable length, nominal diameter, weight, dislocation count, measured lifetime (Westech Lifetime Measurement System), and average resistivity is shown in Table 1. As can be seen, all five ingots had high dislocation densities. Hall samples were prepared from several ingots and subsequently evaluated for room temperature and low temperature mobility in order to verify the purity of the ingot material. These results are presented in Table 2.

At this point several modifications were made in the ion implantation technique which proved beneficial in reducing dislocation densities. First, the stainless steel aperture in the implant apparatus was replaced with a high resistivity silicon aperture. This prevents possible contamination of the ingot by the sputtering of the metal aperture and subsequent imbedding of the sputtered material into the crystal. It is believed that a one order of magnitude reduction in donor concentration can be realized by this modification.<sup>(8)</sup> Secondly, implantation was performed in symmetric quadrants about the ingot axis instead of on one side of the ingot only. This would improve the distribution of the implanted boron in final ingot growth. Thirdly, prior to the final ingot growth pass, a "skin pass" was made with the RF coil in order to anneal out damage caused by the implantation.

Table 1  
ION IMPLANT  
TEST CHARACTERISTICS

Crystal #	Usable Length cm	Nominal Dia. cm	Weight gm	Disloc. Density cm <sup>-2</sup>		Lifetime μs	Ave. Resis. Ω-cm
				Seed	Tang		
F01774503	4.58	3.26	86.1	38,718	$\cdot 10^6$	<10	.19
F01774202	4.15	3.21	77.8	232,000	$\cdot 10^6$	100	2.95
F02774201	5.89	3.20	109.3	37,602	$\cdot 10^6$	80	7.18
F01774703	10.99	2.94	170.2	18,987	$\cdot 10^6$	225	23.64
F10774701	6.00	3.04	99.2	27,550	$\cdot 10^6$	200	24.78
*F01782904	7.30	3.66	172.6	-0-	-	<10	2.00
*F01780604	5.30	3.56	113.4	-0-	-	98	24.40

RECORDED INSTITUTE

Table 2  
DOPING CONCENTRATION

<u>Crystal #</u>	<u>Dopant (1)</u>	<u>Dopant Method</u>	<u>Ave. Resist. cm<sup>-3</sup></u>	<u>Dopant Conc. cm<sup>-3</sup></u>	<u>Donor Conc. cm<sup>-3</sup></u>
			Calcul. Meas.		
F01774503	B	Implant	0.20	0.19	$2.3 \times 10^{17}$
F01774202	B	Implant	2.00	2.90	$8.7 \times 10^{15}$
F02774201 (2)	BF <sub>2</sub>	Implant	2.00	7.20	NA
F01774703	B	Implant	20.00	23.60	NA
F01774701	B	Implant	20.00	24.80	$6.3 \times 10^{14}$
F01782904	B	Implant	2.00	2.00	-
F01780604	B	Implant	20.00	24.00	-

(1) All final doped ingots are p-type

(2) The implanted ion species was BF<sub>2</sub> rather than B

After the above modifications, 2 and 24 ohm-cm, boron doped ingots were successfully grown with zero defects. However, an attempt to grow a 0.2 ohm-cm single crystal proved unsuccessful. After the implant operation on this ingot, the 12 implanted quadrants on the ingot were clearly visible with the naked eye, indicating some type of residue had accumulated in these areas. It is suspected that this residue is caused by the deposition of hydrocarbons from the residual atmosphere in the vacuum system during implantation. Such a layer has been observed after high dose implantation of silicon wafers as well.<sup>(9)</sup> The diffusion pump oil used in the vacuum system is the suspected source of these hydrocarbons. Several growth passes were performed on this ingot, but in each attempt a zero defect single crystal could not be grown.

### 2.3.2.2 Diborane Doping

Diborane doping of pre-purified ingots was performed in the Sieman's Model VZA-3 Float Zone Crystal Grower at Hughes IPD. Welded stainless steel fittings were used in the gas system to avoid contamination of the spectroscopic purity gases used.

A narrow gas stream containing the diborane was directed at the molten zone of the ingot during the float zoning operation. The diborane is subsequently decomposed at the molten zone and the boron is then incorporated into the silicon. The entire chamber is flushed with high purity argon gas during this operation. A final vacuum float zoning was then performed at Great Western Silicon to attain the 1.25 inch diameter, single crystal ingots. Ingots of 2 ohm-cm and 4 ohm-cm resistivities were successfully grown in this manner. These ingots may have been contaminated due to a problem in the system's gas exhaust line or ammonia hydroxide.

An additional ingot was diborane doped to a resistivity of 0.7 ohm-cm. However, attempts to grow this ingot defect free in the final growth pass were unsuccessful. This ingot also exhibited anomalous resistivity measurement readings which could not be explained. Lifetimes of all the diborane doped ingots were too low to measure (< 10  $\mu$ sec) on the equipment available on this program. Hall measurements were not performed on any of the diborane ingots.

#### 2.3.2.3 Gallium Doping

Gallium doping was performed in order to investigate reported radiation resistance properties attributed to silicon doped with this element. The superior lattice match of gallium compared to boron in silicon is certainly one advantage of this dopant. Gallium doping of the float zoned silicon rod was performed at Hughes Research Labs. This was done by introducing the proper amounts of elemental gallium into the seed end of the pre-purified rod, and then zoning through the rod in a single, dislocation-free pass. Zero defect ingots 1.25" in diameter of 0.17, 2, 10 and 20 ohm-cm resistivities were grown in this manner. The only major difficulty encountered in the ingot growth was in the weighing of the minute quantities of gallium ( $\sim$  50  $\mu$ g) needed for the higher resistivity crystals.

Sample wafers were prepared for Hall measurements as well as lifetime measurements (Westech) from these ingots. The results of these measurements are shown in Table 3.

Table 3

LIFETIMES AND IMPURITY CONCENTRATIONS\*  
OF GALLIUM DOPED INGOTS

RESISTIVITY (ohm-cm)	N <sub>BORON</sub> (cm <sup>-3</sup> )	N <sub>GALLIUM</sub> (cm <sup>-3</sup> )	N <sub>DONOR</sub> (cm <sup>-3</sup> )	LIFETIME (μsec)
.17	$2.0 \times 10^{13}$	$2.3 \times 10^{17}$	$0.9 \times 10^{12}$	<10
2	$1.83 \times 10^{12}$	$9.7 \times 10^{15}$	$1.85 \times 10^{12}$	500
10	$3.8 \times 10^{12}$	$2.0 \times 10^{15}$	$2.8 \times 10^{12}$	230
20	$3.3 \times 10^{12}$	$4.0 \times 10^{14}$	$1.2 \times 10^{12}$	10

\*DETERMINED BY HALL EFFECT MEASUREMENTS

The reason for the observed trend of decreasing lifetime as dopant concentration decreases for the 2, 10, and 20 ohm-cm material could not be explained.

### 2.3.3 Crystal Growth Summary

A list of all the crystals grown for this program is presented in Table 4. As can be seen, little problem was encountered in the attainment of zero defect crystals using gallium as the primary dopant. However, the difficulties encountered in the boron doping seriously affected the reliability of further experiments involving these crystals. It is felt that the major obstacle to the successful growth of both the diborane and ion implanted crystals was the difficulty Hughes IRB had in utilizing the Sieman's VZA-3 furnace for the final zoning passes. The inability to utilize an in-house crystal growth facility as planned had several far reaching consequences. These include:

- 1) Major efforts were directed toward modification of the equipment rather than toward improvements in the crystal doping techniques.
- 2) The desired controls on the system cleanliness could not be implemented.
- 3) Schedule slippages in the crystal deliveries resulted in the necessity of using initial experimental crystals for final sample delivery.

Table 4

<u>INGOT #</u>	<u>RESISTIVITY (ohm-cm)</u>	<u>DOPING METHOD</u>	<u>DISLOCATION DENSITY (cm<sup>-2</sup>, seed)</u>	<u>LIFETIME (usec)</u>
1774503	.1	B Implant	38,718	~16
1774202	3	B Implant	232,000	16
2774201	7	BF <sub>2</sub> Implant	37,602	8
1774703	24	B Implant	18,987	22
1774701	25	P Implant	27,550	200
1782904	2	B Implant	-0-	12
1780604	24	B Implant	-0-	9.5
1784003	.2	B Implant	Poly Crystal	-
3796601	.7	Diborane	Poly Crystal	-
1780403	2	Diborane	-0-	~11
3796602	4	Diborane	-0-	10
1775001	.17	Gallium	-0-	10
1783302	2	Gallium	-0-	500
1780302	10	Gallium	-0-	230
1783002	20	Gallium	-0-	10

## 2.4 MATERIAL EVALUATIONS

Final material evaluations consisted of the following:

- 1) Fabricate solar cells
- 2) Measure electrical characteristics (I-V curves)
- 3) Irradiate samples (electrons)
- 4) Remeasure electrical characteristics (I-V curves)
- 5) Check photon stability of devices post electron irradiation.

The results of these studies are described in the following sections.

### 2.4.1 Cell Processing

All of the various crystal types successfully grown were sliced into approximately 470 micron thick wafers. Cells were then fabricated as follows:

- 1) Chemical polish wafers (300 microns thick)
- 2) PNH clean
- 3) PH<sub>3</sub> diffuse wafers - 825°C (Sheet resistivity ~ 100 ohms/square)
- 4) Dice into 2 x 2 cm cells
- 5) Back etch
- 6) Evaporate rear contact (Ti-Ag)
- 7) Contact sinter (600°C)
- 8) Evaporate front contact grid pattern (Ti-Ag)
- 9) Apply Ta<sub>2</sub>O<sub>5</sub> AR coating

The PNH cleaning technique uses a sequence of ammonium hydroxide, hydrogen peroxide, hydrochloric acid, and hydrofluoric acid to provide a wafer with a highly cleaned surface. The "N" contact structure consisted of twenty-four, 0.025 mm wide Ti-Ag grid fingers attached to an ohmic bar. The above process sequence yields a very basic N<sup>+</sup>/P solar cell structure. No attempt at process optimization was made for these studies.

#### 2.4.2 Electrical Evaluation

After cell fabrication, AM0 electrical data was obtained using a Spectrosun X-25 solar simulator. Data is presented for the boron doped cells in Table 5, and for the gallium doped cells in Table 6. In each case, cells made from conventional, boron doped CZ material were processed along with the test material. These tables represent average data for the ten to twenty cells processed of each cell type.

In Table 5 there seems to be no clear advantage in electrical performance of the implanted material over the conventional CZ control cells. However, the diborane results are of some interest. Although the 2 ohm-cm diborane material shows very poor open circuit voltages, the higher resistivity, 4 ohm-cm material exhibits a higher V<sub>oc</sub> than any of the 2 ohm-cm boron doped material. The 2, 10, and 20 ohm-cm gallium doped material shows no marked improvement in open circuit voltage or short circuit current over the conventional CZ controls in Table 6.

Although the curve shape of the control cells is poor in this table, the V<sub>oc</sub>'s and the I<sub>sc</sub>'s of these samples are fairly typical of the resistivity ranges.

Table 5

AVERAGE 25°C AMO ELECTRICAL DATA  
BORON DOPED CELLS, 300 MICRONS THICK

<u>INGOT #</u>	<u>BASE RESISTIVITY</u>	<u>DOPING METHOD</u>	<u>V<sub>OC</sub></u> (mV)	<u>I<sub>SC</sub></u> (mA)	<u>P<sub>max</sub></u> (mW)	<u>FF</u>
1774503	0.1	Implant	625	140	67.4	.77
1782904	2	Implant	591	143	67.7	.80
1780403	2	Diborane	577	144	65.3	.79
3790602	4	Diborane	593	143	67.0	.76
1780604	24	Implant	525	146	59.4	.77
	2	CZ Controls	593	140	64.9	.78
	10	CZ Controls	542	140	59.4	.78

Table 6

AVERAGE AMO ELECTRICAL DATA  
GALLIUM DOPED MATERIAL, 300 MICRONS THICK

<u>INGOT #</u>	<u>BASE RESISTIVITY</u>	<u>V<sub>OC</sub></u> (mV)	<u>I<sub>SC</sub></u> (mA)	<u>P<sub>max</sub></u> (mW)	<u>FF</u>	<u>TEST TEMP</u>
1775001	0.17	632	146	73.3	.79	25°C
1783302	2	582	145	64.7	.77	28°C
1780502	10	544	148	61.8	.77	28°C
1782002	20	514	147	55.0	.75	28°C
	2 (Boron CZ)	582	146	59.7	.71	28°C
	10 (Boron CZ)	531	150	62.6	.76	28°C

Of particular interest in Table 6 is the performance of the 0.17 ohm-cm gallium doped material. Several of the cells in this group had open circuit voltages at 25°C of 633 mV. This value is the highest open circuit voltage measured to date at Spectrolab on a non-back surface field cell. Also of interest is the high short circuit current of these cells, as well as the excellent curve fill factors. The best cell of the group had a power of 74.7 mW, or 13.8% efficiency. This is extremely good, keeping in mind the rather simple, unoptimized cell processing used on these devices.

#### 2.4.3 Electron Irradiation Tests

Several cells from each group processed were sent to the JPL Dynamitron facility for electron irradiation tests. All cells were irradiated to a fluence level of  $3 \times 10^{14}$  e/cm<sup>2</sup> and the gallium doped cells were irradiated to a fluence level of  $1 \times 10^{15}$  e/cm<sup>2</sup>. The diborane and the boron implant cells were annealed at 60°C for 48 hours and the gallium doped cells were annealed at 60°C for approximately 17 hours after each irradiation. The results of the  $3 \times 10^{14}$  e/cm<sup>2</sup> fluence level is given in Table 7. The results of  $1 \times 10^{15}$  e/cm<sup>2</sup> fluence level is given in Table 8. Data has been given in terms of normalized short circuit current, open circuit voltage, and maximum power. Also included in Tables 7 and 8 are data for 2 and 10 ohm-cm shallow junction devices as presented in the JPL Solar Cell Radiation Handbook<sup>(11)</sup>.

All of the two ohm-cm material studied showed slight improvement in radiation hardness over the conventional CZ 2 ohm-cm control cells. This could be attributed to the improved purity of these crystals. However, the 4 ohm-cm diborane, 10 and 20 ohm-cm gallium, and 24 ohm-cm implant cells show no improvement over conventional CZ material.

Table 7

ELECTRON IRRADIATION DATA  
 $3 \times 10^{14}$  e/cm<sup>2</sup>, 1 MeV ELECTRONS

<u>CELL TYPE/DOPANT</u>	<u>P/P<sub>O</sub></u>	<u>V/V<sub>O</sub> (Oc)</u>	<u>I/I<sub>O</sub> (Sc)</u>
2 ohm B Implant	.805	.940	.875
2 ohm Diborane	.857	.946	.903
2 ohm CZ Boron	.796	.938	.857
4 ohm Diborane	.801	.941	.862
10 ohm CZ Boron	.863	.957	.936
0.1 ohm B Implant	.732	.947	.736
0.17 Ohm Gallium	.761	.950	.807
2 ohm Gallium	.815	.951	.878
10 ohm Gallium	.871	.968	.918
20 ohm Gallium	.896	.981	.945
24 ohm B Implant	.830	.970	.950
*2 ohm CZ Boron	.810	.935	.870
*10 ohm CZ Boron	.860	.955	.920

\*JPL Radiation Handbook Data<sup>(11)</sup>

Table 8

ELECTRON IRRADIATION DATA  
 $1 \times 10^{15} \text{ e/cm}^2$ , 1 MeV ELECTRONS

<u>CELL TYPE/DOPANT</u>	<u>P/P<sub>O</sub></u>	<u>V/V<sub>O</sub>(OC)</u>	<u>I/I<sub>O</sub>(SC)</u>
0.17 ohm Gallium	.648	.928	.717
2 ohm Gallium	.722	.920	.792
10 ohm Gallium	.776	.930	.852
20 ohm Gallium	.810	.955	.886
2 ohm CZ Boron	.719	.910	.794
10 ohm CZ Boron	.760	.934	.849
*2 ohm CZ Boron	.720	.905	.805
*10 ohm CZ Boron	.770	.920	.865

\*JPL Radiation Handbook Data<sup>(1)</sup>

The radiation stability of the 0.17 ohm-cm gallium material is of interest however. This material's radiation hardness is very close to that of the 2 ohm-cm CZ material after  $3 \times 10^{14}$  e/cm<sup>2</sup>. This should be compared to the relatively poor showing of the 0.1 ohm-cm boron implant doped cells. Another comparison can be made with work presented by NASA-Lewis Research Center<sup>(10)</sup> as illustrated in Figure 4. In this figure normalized short circuit current versus electron fluence for several advanced types of low resistivity, 0.1 ohm-cm boron doped cells, including high-low emitter cells, diffused junction cells and ion-implanted junction cells are presented. Also indicated is data obtained for the 0.17 ohm-cm gallium doped material after  $3 \times 10^{14}$  e/cm<sup>2</sup> and after  $1 \times 10^{15}$  e/cm<sup>2</sup>. Again note the improvement in the gallium doped material.

#### 2.4.4 Photon Degradation Experiments

It has been shown that irradiated float zone grown, low resistivity boron doped silicon cells show additional electrical degradation after photon irradiation. In order to check this effect, cells were placed under a xenon light source for 10 hours after electron irradiation, and then remeasured electrically. Normalized maximum power values both directly after irradiation and after 10 hours of illumination are given in Table 9. Note the large additional degradation of the boron implanted cells. Similar degradation was observed qualitatively on the 2 ohm-cm diborane doped material as well. However, the gallium doped material remained quite stable under photon illumination.

#### 2.4.5 Material Evaluation Summary

Of the material studied, by far the most interesting was the 0.17 ohm-cm gallium doped silicon. Cells fabricated from this

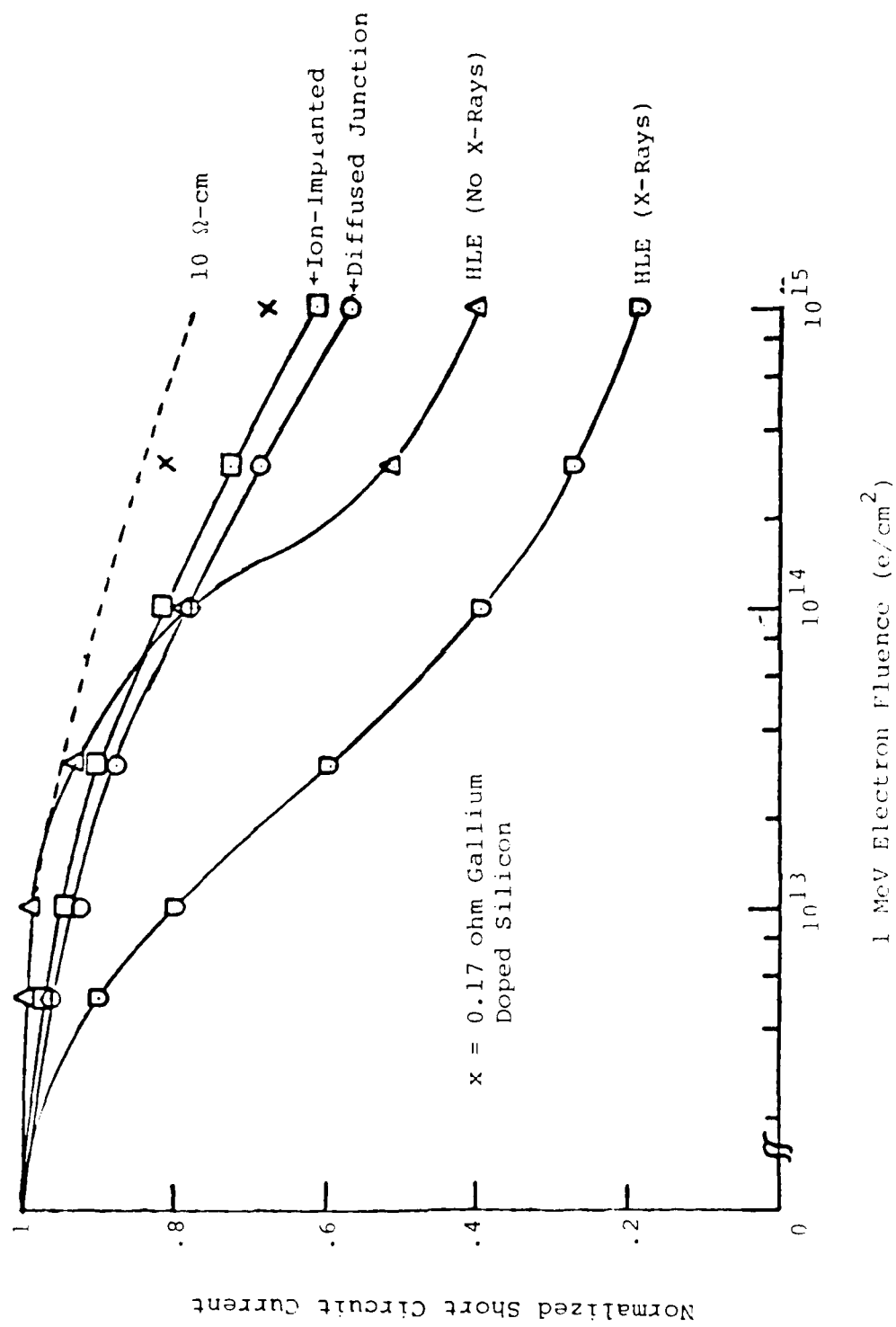


FIGURE 4. NORMALIZED  $I_{sc}$  VS ELECTRON FLUENCE  
(0.1 ohm Boron Doped Material)

Table 9

PHOTON DEGRADATION EXPERIMENT  
 POST  $3 \times 10^{14}$  e/cm<sup>2</sup>

<u>CELL TYPE</u>	<u>P/P<sub>0</sub></u> $(3 \times 10^{14}$ e/cm <sup>2</sup> )	<u>P/P<sub>0</sub></u> $(3 \times 10^{14}$ e/cm <sup>2</sup> + 10 HOURS PHOTON)
2 ohm B Implant	.821	.728
.1 ohm B Implant	.752	.652
2 ohm B CZ	.789	.770
0.17 ohm Gallium	.763	.751
2 ohm Gallium	.815	.818

material indicated the potential of high power levels, with the achievement of open circuit voltages of 633 mV at 25°C, AM0, on standard N<sup>+</sup>/P devices. The data also indicated enhanced radiation stability of this material over boron doped, low resistivity material. There was no tendency for the Si:Ga cells to further degrade upon exposure to photon irradiation, a result which is in contrast to the large degradation observed on the other float zone grown materials studied.

## 2.5 PROCESS OPTIMIZATION - GALLIUM DOPED MATERIAL

The materials evaluation phase of this program indicated that float zone grown silicon solar cells doped with gallium may have improved tolerance to electron irradiations over cells fabricated from boron doped material. However, this evaluation was based on cells fabricated using standard N<sup>+</sup>/P processing. The question then arose: Would this trend be observed in cells processed using high efficiency process techniques? Though cell process optimization was beyond the scope of this contract, Spectrolab's internal efforts in this direction are pertinent to the conclusions of this program.

### 2.5.1 (100) Oriented Si:Ga Ingot

All of the material studied on this contract was (111) oriented, "P" type silicon. However, advanced processing techniques, such as texturizing the front surfaces, are only possible using (100) oriented wafers. Therefore, an additional ingot was supplied to Spectrolab by Hughes IPD which was 2 ohm-cm gallium doped with (100) orientation. This ingot (F01791005) was subsequently sliced and then fabricated into solar cells using the most sophisticated processing techniques available to Spectrolab at the time, those

developed on the HESP II program (Air Force Contract No. F33615-77-C-3108). Both 0.008" thick and 0.002" thick cells were processed, all cells featuring textured front surfaces, aluminum paste back surface fields, and  $Ta_2O_5$  AR coatings. The 25°C, AM0 data of the cells processed are shown in Table 10. Though the number of cells processed was small, the ability to fabricate high efficiency cells using the silicon doped with gallium is evident.

#### 2.5.2 Electron Irradiation Test

Two cells were chosen from each of the high efficiency cell thickness groups for 1 MeV electron irradiations. The cells were then irradiated to fluence levels of  $3 \times 10^{14}$  and  $1 \times 10^{15}$  e/cm<sup>2</sup>. The results of this test are summarized in Table 11. The performance of textured, boron doped cells developed on the HESP II program and results on Spectrolab's 0.002" thick cell development programs are also included for comparison. Boron doped samples were all from CZ grown material. Though the sample size is again extremely small, the data indicates that the 2 ohm-cm gallium doped cell's performance is equal to or somewhat superior to the 10 ohm-cm boron doped cells after electron irradiations. In addition, the gallium doped high efficiency cells showed no tendency to further degrade after electron irradiations when exposed to photons.

Table 10

25<sup>0</sup>C, AMO TEST DATA - (100), 2 ohm-cm  
GALLIUM DOPED MATERIAL

LOT - CELL	V <sub>OC</sub> mV	I <sub>SC</sub> mA	V <sub>mp</sub> mV	I <sub>mp</sub> mA	P <sub>max</sub> mW	CFP	EFF %
<u>8 mil Cells</u>							
2 - 1	610	172	510	157	80.1	.76	14.8
2	611	172	520	160	83.2	.79	15.4
3	610	174	518	155	80.3	.76	14.8
4	610	172	518	161	83.4	.79	15.4
5	612	173	518	163	84.4	.80	15.6
<u>2 mil Cells</u>							
4 - 1	616	167	512	157	80.4	.78	14.9
2	618	169	512	157	80.4	.77	14.9
3	612	168	500	157	78.5	.76	14.5
4	610	170	520	156	81.1	.78	15.0
5	613	172	508	162	82.3	.78	15.2
6	614	170	508	158	80.3	.77	14.8
7	618	170	518	158	81.8	.78	15.1

Table 11

25°C, AM0 ELECTRON IRRADIATION DATA  
HIGH EFFICIENCY CELLS

<u>CELL TYPE</u>	<u><math>P_O^*</math> (mW)</u>	<u><math>P_3 \times 10^{14}</math> (mW)</u>	<u><math>\frac{P_3 \times 10^{14}}{P_O}</math></u>	<u><math>P_1 \times 10^{15}</math> (mW)</u>	<u><math>\frac{P_1 \times 10^{15}}{P_O}</math></u>
2 ohm, Gallium 8 mil	83.1	65.3	.786	56.5	.680
2 ohm, Gallium 2 mil	79.0	68.6	.868	59.4	.751
10 ohm, Boron 8 mil	84.1	65.6	.780	56.3	.669
10 ohm, Boron 2 mil	75.4	64.9	.861	59.2	.785

\*Average power of cells irradiated - All cells w/BSF and textured front surface

### 3.0 CONCLUSION

In this program an attempt was made to improve both silicon solar cell beginning-of-life power and end-of-life power through the development of improved lifetime, high purity material. The methods chosen for study included:

- 1) Gettering of impurities from conventional CZ grown silicon wafers.
- 2) Float zone growth of ingots doped with boron using ion implantation.
- 3) Float zone growth of ingots doped with boron using diborane gas under extremely clean conditions.
- 4) Float zone growth of ingots doped with gallium.

Cells fabricated from the gettered material and from the boron doped float zone material showed no performance advantages over cells fabricated from conventional CZ grown material. However, problems with the ingot growth and hence possible crystal contamination cast serious doubt on the cell evaluations of the float zone grown material doped either by ion implantation or diborane gas.

By contrast, the performance of cells float zone grown with gallium as a dopant were quite promising. Open circuit voltages of 633 mV with AM0 conversion efficiencies approaching 14% were achieved with low resistivity, 0.17 ohm-cm gallium doped material using standard N<sup>+</sup>/P type processing. In addition, electron irradiation testing on this material indicated enhanced end-of-life characteristics as well, with no tendency to further degrade under illumination post electron irradiation.

This program has therefore demonstrated that high efficiency solar cells can be fabricated using high purity float zone grown, gallium doped silicon which has no tendency to degrade when exposed to photons after electron irradiation as has been commonly observed using float zone grown, boron doped material. This result has brought up a basic question, however. Is the improved performance of the Si:Ga material a result of reduced impurity levels due to the method of crystal growth, or is gallium an inherently better dopant than boron for low resistivity solar cells. In further studies involving high purity material the need exists, therefore, for the ability to identify low concentration impurities, and also to identify when such impurities are introduced, i.e., in the initial polycrystalline silicon, during crystal growth, or during cell processing. Advanced diagnostic methods must therefore be utilized. One technique which may prove useful in this regard is DLTS (Deep Level Transient Spectroscopy) which has the demonstrated ability to identify trap levels in silicon before, during, and after processing with a sensitivity level of  $10^{10} \text{ cm}^{-3}$ .

## REFERENCES

- 1) Fodor, J. and Opjorden, R., High Efficiency Solar Panel, Phase II, WPAFB Contract No. F33615-77-C-3108, to be published.
- 2) Wolf, M. "Updating The Limit Efficiency of Silicon Solar Cells", NASA-Lewis Publication No. 2097, Solar Cell, High Efficiency and Radiation Damage, 1979, pp 15-28.
- 3) Wysocki, J.J. and Rappaport, P., J. Appl. Physics, Volume 31, 1960, p. 571.
- 4) Meek, R.L., Buck, T.M., and Biggon, C.F., "Silicon Surface Contamination; Polishing and Cleaning", J. Electrochem. Soc. Volume 120, No. 9, p. 1241.
- 5) Scott-Monck, J.A., Stella, P. and Avery, J., "Development of Processing Procedures for Advanced Silicon Solar Cells", Final Report NASA CR-134740, Jan. 1975.
- 6) Scott-Monck, J. and Stella, P., "Textured Surface Cell Performance Characteristics", 12th Photovoltaic Specialists Conference Record, p. 600, 1976.
- 7) MacIver, B.A., J. Electrochem. Soc. Solid State Science and Technology, February 1977, pp. 273-275.
- 8) Haas, E.W. et al, J. of Elect. Materials, Volume 7, 1978, pp. 525-533.
- 9) Tasi, M.Y. et al, J. Electrochem. Soc. Solid State Science and Technology, Jan. 1979, pp. 98-102.
- 10) Weinberg, I. et al, "Radiation Damage in High Voltage Silicon Solar Cells", NASA-Lewis Publication No. 2097, Solar Cell, High Efficiency and Radiation Damage, 1979, pp. 137-143.
- 11) Tada, H.Y. and Carter, J.R., Solar Cell Radiation Handbook, JPL Publication 77-56, Nov. 1, 1977, pp. 3-79 to 3-98.

